Solitary solutions of the Schrödinger-Poisson equations in one and two dimensions

Gin-yih Tsaur*

Abstract

The Schrödinger-Poisson equations are a set of nonlinear equations that form the back-bone of many important physics problems. An interesting problem is the effect of gravity in quantum mechanics. The density distribution described by the wavefunction ψ produces a gravitational potential V through the Poisson equation, and the potential V in turn changes the wavefunction ψ itself through the Schrödinger equation. Such a feedback mechanism provides a nonlinear effect that leads to solitary solutions. In this paper 1-D and 2-D solitary solutions of the Schrödinger-Poisson equations are computed by both the shooting method and the boundary-value method. The shooting method is efficient for finding solutions in the short range, but unstable in the long range. Whereas, long-range solutions can be computed accurately by the boundary-value method with the short-range initial guess provided by the shooting method. Hence for this problem these two methods play complementary roles in the numerical computation.

1   Introduction

The Schrödinger-Poisson equations can be written as

$$i\frac{\partial}{\partial t}\psi_i = -\nabla^2\psi_i + V\psi_i, \quad \nabla^2 V = \sum_i |\psi_i|^2 \tag{1.1}$$

for gravitational systems, or

$$i\frac{\partial}{\partial t}\psi_i = -\nabla^2\psi_i + q_i V\psi_i, \quad -\nabla^2 V = \sum_i q_i |\psi_i|^2 \tag{1.2}$$

for electrical systems, where q_i represents the charge of the ith species of particle. The first part in Eqs. (1.1) and (1.2) is the Schrödinger equation, in which the probability amplitude ψ_i is determined by the potential V, and the second part is the Poisson equation, in which the potential V is induced by the probability densities $|\psi_i|^2$ of all the particles. Applications of the Schrödinger-Poisson equations includes modelling self-gravitating systems such as bosonic stars [1–4], and

*Department of Mathematics, Tunghai University, Taichung 407, Taiwan

modelling the Coulomb interaction between charge carriers in semiconductors [5–9]. In general, the Schrödinger-Poisson equations can be considered as a quantum version of the Vlasov-Poisson equations or a statistical version of the Hartree-Fock equations, both of them have a wide range of applications in physics.

If only a single species of particle is considered, Equations (1.1) and (1.2) can be rescaled to

$$i\frac{\partial}{\partial t}\psi = -\nabla^2\psi + V\psi, \quad -\varepsilon\nabla^2 V = |\psi|^2, \tag{1.3}$$

where $\varepsilon = -1$ when the force is attractive and $\varepsilon = +1$ when the force is repulsive. Equation (1.3) has a unique global solution with the initial condition

$$\psi(\boldsymbol{x}, t=0) = \psi_0(\boldsymbol{x}), \tag{1.4}$$

and the boundary condition

$$\lim_{|\boldsymbol{x}|\to\infty}\psi = \lim_{|\boldsymbol{x}|\to\infty} V = 0, \tag{1.5}$$

if the initial data $\psi_0(\boldsymbol{x})$ is an $H^2(\mathbb{R}^3)$ function [10]. These solutions are generally not stationary. For the repulsive case ($\varepsilon = +1$) with finite energy, the solutions decay asymptotically to zero as $t \to \infty$ [10–12]. Similarly, for the attractive case ($\varepsilon = -1$) with positive energy, the solutions expand unboundedly as $t \to \infty$ [13,14]. Only for the attractive case with negative energy, stationary 3-D solutions exist [14]. In this case there exists an infinite family of stationary normalizable spherically-symmetric solutions [15]. The first tens of them have been computed explicitly by the shooting method [3,16] or by the boundary-value method [17], and some analytical justifications for the numerical results can be found in [15,18]. In this paper the focus is on the attractive case in 1 and 2 dimensions. We compute the stationary normalizable symmetric solutions in Secs. 2, 3 and study the convergence of the solutions at large r in Sec. 4.

For the attractive case, Eq. (1.3) becomes

$$i\frac{\partial}{\partial t}\psi = -\nabla^2\psi + V\psi, \quad \nabla^2 V = |\psi|^2. \tag{1.6}$$

The equation is satisfied by the stationary solutions $\psi(\boldsymbol{x}, t) = e^{-i\omega t}\Psi(\boldsymbol{x})$, $V = V(\boldsymbol{x})$ or the solitary solutions $\psi(\boldsymbol{x}, t) = e^{-i\omega t}e^{i(\boldsymbol{v}\cdot\boldsymbol{x}/2 - v^2 t/4)}\Psi(\boldsymbol{x} - \boldsymbol{v}t)$, $V = V(\boldsymbol{x} - \boldsymbol{v}t)$ with arbitrary velocity $\boldsymbol{v}$, when Ψ and V satisfy

$$\nabla^2\Psi = (V - \omega)\Psi, \quad \nabla^2 V = \Psi^2. \tag{1.7}$$

Since stationary and solitary solutions are related simply by a change of reference frame, we shall not distinguish them in the rest of this paper. In the 1-D and 2-D cases, the equations for symmetric solutions are respectively

$$\Psi_{rr} = (V - \omega)\Psi, \quad V_{rr} = \Psi^2, \tag{1.8-1}$$

$$(r\Psi_r)_r = r(V - \omega)\Psi, \quad (rV_r)_r = r\Psi^2. \tag{1.8-2}$$

The smoothness of the solutions at $r = 0$ is required,

$$\Psi_r(0) = 0, \quad V_r(0) = 0, \tag{1.9}$$

and the normalization condition is also required, which is respectively

$$\int_0^\infty \Psi^2 dr = 1, \tag{1.10-1}$$

$$\int_0^\infty 2\pi r \Psi^2 dr = 1. \tag{1.10-2}$$

By integrating the the Poisson equations in Eq. (1.8) with respect to r, and substituting in $V_r(0) = 0$, it is seen that Eq. (1.10) is equivalent to the boundary conditions

$$V_r \to 1 \quad \text{as} \quad r \to \infty, \tag{1.11-1}$$

$$rV_r \to \frac{1}{2\pi} \quad \text{as} \quad r \to \infty, \tag{1.11-2}$$

namely

$$V \to r \quad \text{as} \quad r \to \infty, \tag{1.12-1}$$

$$V \to \frac{\ln r}{2\pi} \quad \text{as} \quad r \to \infty. \tag{1.12-2}$$

The integration constant in Eq. (1.12) is not important because the solution can be changed to $V + c$ for any constant c with the eigenvalue changed to $\omega + c$. In section 2 we search for the solutions of Eqs. (1.8), (1.9), (1.10) using the shooting method and in section 3 Eqs. (1.8), (1.9), (1.12) using the boundary-value method. Because for large r the shooting method becomes extremely sensitive to the initial value, it can only provide solutions in a limited range. The boundary-value method is used to verify the solutions and extend them to large r where the shooting method is inherently unstable.

2   Solutions by the Shooting Method

Let us define a new variable Y by

$$Y \equiv V - \omega. \tag{2.1}$$

In terms of Y, Eqs. (1.8) and (1.9) become

$$\Psi_{rr} = Y\Psi, \quad Y_{rr} = \Psi^2, \tag{2.2-1}$$

$$(r\Psi_r)_r = rY\Psi, \quad (rY_r)_r = r\Psi^2, \tag{2.2-2}$$

and

$$\Psi_r(0) = 0, \quad Y_r(0) = 0. \tag{2.3}$$

Since Eqs. (2.2), (2.3), and the normalization condition Eq. (1.10) are invariant under the transformation $\Psi \to -\Psi$, we may assume $\Psi(0) > 0$. If furthermore $Y(0) \geq 0$, then Eqs. (2.2) and (2.3) imply $\Psi_r > 0$, $Y_r > 0$ for all $r > 0$, and $\Psi \to \infty$, $Y \to \infty$ as $r \to \infty$, which violates the normalization condition. Therefore one must have $Y(0) < 0$, namely $\Psi(0)Y(0) < 0$. Hence one has $\Psi Y < 0$ near $r = 0$ and $\Psi^2 \geq 0$ for all r. This implies from Eqs. (2.2) and (2.3) that $\Psi_r < 0$ near $r = 0$ and $Y_r > 0$ for all $r > 0$. Namely Ψ is decreasing when r is small and Y is increasing for all r. From Eqs. (1.12) and (2.1), Y increases

$$\text{from} \quad Y(0) < 0 \quad \text{to} \quad r - \omega \quad \text{as} \quad r \to \infty \tag{2.4-1}$$

for the 1-D case and

$$\text{from} \quad Y(0) < 0 \quad \text{to} \quad \frac{\ln r}{2\pi} - \omega \quad \text{as} \quad r \to \infty, \tag{2.4-2}$$

for the 2-D case.

The Schrödinger equations in Eq. (2.2) are equivalent to

$$\Psi_{rr} = Y\Psi, \tag{2.5-1}$$

$$(\sqrt{r}\Psi)_{rr} = [Y - 1/(4r^2)](\sqrt{r}\Psi), \tag{2.5-2}$$

for the 1-D and 2-D cases respectively. Eq. (2.4) implies that Y for the 1-D case or $Y - 1/(4r^2)$ for the 2-D case are increasing from being negative near $r = 0$ to a transition point $r = r_M$ beyond which they are positive. Therefore Eq. (2.5) implies that the solutions Ψ for the 1-D case or $\sqrt{r}\Psi$ for the 2-D case are oscillatory for $r < r_M$ and either decay to zero faster than some exponentially decaying functions or diverge to $\pm\infty$ faster than some exponentially growing functions for $r > r_M$. Generally the solutions diverge to $\pm\infty$. For every $\Psi(0)$, only a discrete set of special $Y(0)$ makes the solutions decay to zero. The shooting method finds these special $Y(0)$ by successively narrowing down the range (c_1, c_2) in which $Y(0) = c_1$ and $Y(0) = c_2$ cause Ψ to diverge in the opposite directions. Namely, one causes $\Psi \to +\infty$ and the other causes $\Psi \to -\infty$ at large r. By the continuity condition [15], there exists a value of $Y(0)$ in the interval (c_1, c_2) for which Ψ or $\sqrt{r}\Psi$ decay to zero faster than some exponentially decaying functions, and then the integrals $\int_0^\infty \Psi^2 dr$ or $\int_0^\infty 2\pi r \Psi^2 dr$ are finite. These solutions are called the bound-state solutions.

If $\Psi(r)$ and $Y(r)$ satisfy Eqs. (2.2) and (2.3),

$$\widetilde{\Psi}(r) = \frac{1}{\lambda^2}\Psi\left(\frac{r}{\lambda}\right), \quad \widetilde{Y}(r) = \frac{1}{\lambda^2}Y\left(\frac{r}{\lambda}\right), \tag{2.6}$$

also do, where λ is an arbitrary scaling constant. Therefore one can choose a λ to make $\widetilde{\Psi}(r)$ satisfy the normalization condition. As we shall see, the scaling constant λ and the eigenvalue ω can be obtained by fitting the values of the bound-state solutions Y at large r.

2.1 The 1-dimensional case

Because Ψ can be rescaled by Eq. (2.6) to satisfy the normalization condition, one may start the search with $\Psi(0) = 1$. As shown in Fig. 2.1, for $Y(0) = -0.641684$, Ψ has no zeros and approaches $+\infty$, and for $Y(0) = -0.641685$, Ψ has a single zero and approaches $-\infty$. Therefore there exists a value of $Y(0)$ in the interval $(-0.641685, -0.641684)$ for which Ψ has no zeros and decays to zero. By successively narrowing down the interval, the value $Y(0)$ for the ground-state solution is computed to the 14th digit in Fig. 2.1. For $n = 0, 1, 2, 3, 4, 5$, in Fig. 2.2 one can find a value of $Y(0)$ for which Ψ has n zeros and approaches $(-1)^n\infty$, and a nearby lower value of $Y(0)$ for which Ψ has $n+1$ zeros and approaches $(-1)^{n+1}\infty$. Therefore in between these two values there is a $Y(0)$ for which Ψ has n zeros and decays to zero.
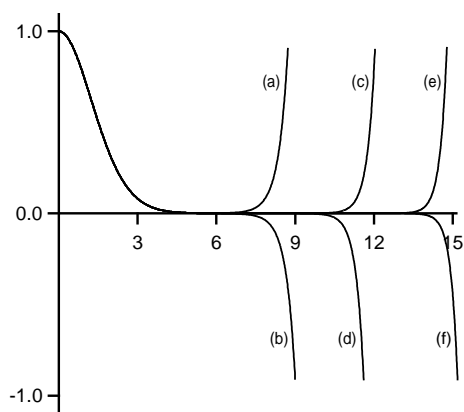

Figure 2.1: the solutions Ψ of Eqs. (2.2-1) and (2.3) with $\Psi(0) = 1$ and $Y(0) = $ (a) -0.641684, (b) -0.641685, (c) -0.641686897, (d) -0.641686898, (e) -0.64168689718419, (f) -0.64168689718420

The values $Y(0)$ for the nth bound-state solution are reported to the fifth digit in the first column of Table 1. With these values the solution Ψ decays to zero faster than some exponentially decaying function, therefore the probability $\int_0^\infty \Psi^2 dr$ is finite. Let

$$\int_0^\infty \Psi^2 dr = \lambda^3, \tag{2.7}$$

then set

$$\widetilde{\Psi}(r) = \frac{1}{\lambda^2}\Psi\left(\frac{r}{\lambda}\right), \quad \widetilde{Y}(r) = \frac{1}{\lambda^2}Y\left(\frac{r}{\lambda}\right), \tag{2.8}$$
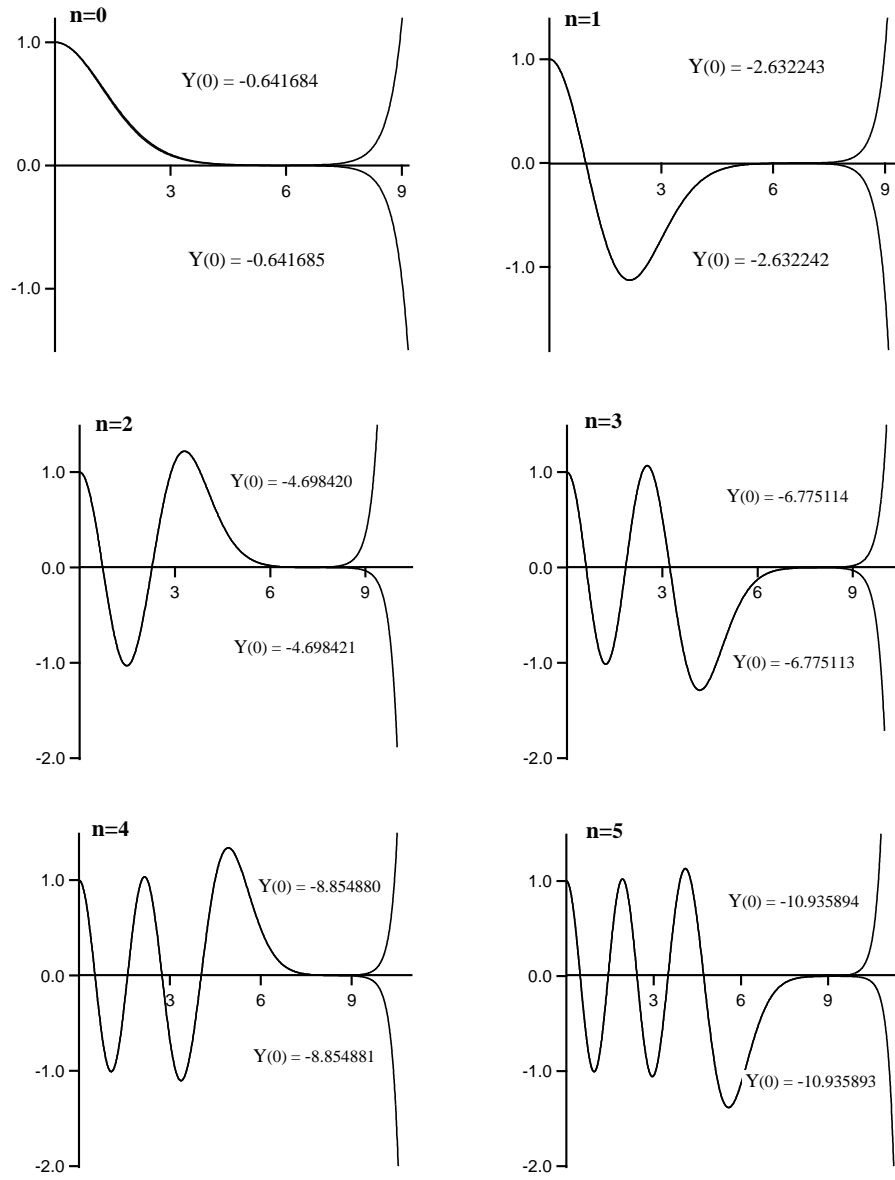
Figure 2.2: the solutions Ψ of Eqs. (2.2-1) and (2.3) with $\Psi(0) = 1$

one can easily check that $\widetilde{\Psi}$ and $\widetilde{Y}$ satisfy Eq. (1.10-1) in addition to Eqs. (2.2-1) and (2.3). Hence

$$\widetilde{Y}(r) \to r - \omega \text{ as } r \to \infty. \tag{2.9}$$

Table 1: Values of $Y_n(0)$, A_n, and B_n for the 1-D case

n	$Y_n(0)$	A_n	B_n
0	-0.64168	1.13286	-1.47076
1	-2.63224	2.29445	-6.95298
2	-4.69842	3.06543	-12.4960
3	-6.77511	3.68106	-18.0465
4	-8.85488	4.20830	-23.5989
5	-10.93589	4.67673	-29.1520

Table 2: Values of λ_n, ω_n, $\widetilde{\Psi}_n(0)$, and $\widetilde{V}_n(0)$ for the 1-D case

n	$\lambda_n = A_n^{1/3}$	$\omega_n = -B_n A_n^{-2/3}$	$\widetilde{\Psi}_n(0) = A_n^{-2/3}$	$\widetilde{V}_n(0) = [Y_n(0) - B_n]A_n^{-2/3}$
0	1.0425	1.3534	0.9202	0.7629
1	1.3189	3.9969	0.5748	2.4837
2	1.4527	5.9217	0.4739	3.6952
3	1.5440	7.5697	0.4195	4.7278
4	1.6145	9.0536	0.3836	5.6565
5	1.6723	10.4241	0.3576	6.5137

From $Y(r) = \lambda^2 \widetilde{Y}(\lambda r)$, one has

$$Y(r) \to Ar + B \quad \text{as } r \to \infty, \tag{2.10}$$

where

$$A = \lambda^3, \quad B = -\lambda^2 \omega. \tag{2.11}$$

Since A and B can be obtained by fitting the values of the bound-state solutions Y at large r, one obtains the scaling constant λ and the eigenvalue ω. The values A and B for the n-th bound-state solution, $n = 0, 1, 2, 3, 4, 5$, are reported in the 2nd and 3rd columns of Table 1. From Eq. (2.11) and $\Psi(0) = 1$, one has

$$\lambda = A^{1/3}, \tag{2.12}$$

$$\omega = -\frac{B}{\lambda^2} = -BA^{-2/3}, \tag{2.13}$$

$$\widetilde{\Psi}(0) = \frac{1}{\lambda^2}\Psi(0) = A^{-2/3}, \tag{2.14}$$

$$\widetilde{Y}(0) = \frac{1}{\lambda^2}Y(0) = Y(0)A^{-2/3}. \tag{2.15}$$

Moreover, in accordance with Eq. (2.1), $\widetilde{V} \equiv \widetilde{Y} + \omega$, one has

$$\begin{aligned}\widetilde{V}(0) &= \widetilde{Y}(0) + \omega \\ &= [Y(0) - B]A^{-2/3}.\end{aligned} \tag{2.16}$$

The values λ, ω, $\widetilde{\Psi}(0)$, $\widetilde{V}(0)$ for the n-th bound-state solution, $n = 0,1,2,3,4,5$, are reported in Table 2. They will be used in the initial guess for the boundary-value method in Section 3.

2.2 The 2-dimensional case

Similar to the 1-D case, we start the search with $\Psi(0) = 1$ and estimate the value $Y(0)$ for the ground-state solution to the 14th digit in Fig. 2.3. The values $Y(0)$ for the n-th bound-state solutions, $n = 0,1,2,3,4,5$, are shown in Fig. 2.4 and reported in the first column of Table 3 to the fifth digit.
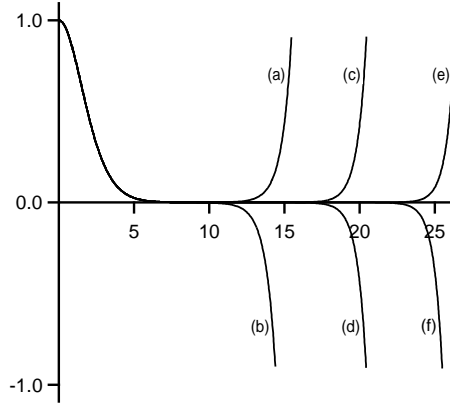

Figure 2.3: the solutions Ψ of Eqs. (2.2-2) and (2.3) with $\Psi(0) = 1$ and $Y(0) =$ (a) -0.824107, (b) -0.824108, (c) -0.8241071603, (d) -0.8241071604, (e) -0.82410716034937, (f) -0.82410716034938

With these values the solution $\sqrt{r}\Psi$ decays to zero faster than some exponentially decaying function, therefore the probability $\int_0^\infty 2\pi r^2 \Psi^2 dr$ is finite. Let

$$\int_0^\infty 2\pi r \Psi^2 dr = \lambda^2, \tag{2.17}$$

then set

$$\widetilde{\Psi}(r) = \frac{1}{\lambda^2}\Psi\left(\frac{r}{\lambda}\right), \quad \widetilde{Y}(r) = \frac{1}{\lambda^2}Y\left(\frac{r}{\lambda}\right), \tag{2.18}$$

one can easily check that $\widetilde{\Psi}$ and $\widetilde{Y}$ satisfy Eq. (1.10-2) in addition to Eqs. (2.2-2) and (2.3). Hence

$$\widetilde{Y}(r) \to \frac{\ln r}{2\pi} - \omega \text{ as } r \to \infty. \tag{2.19}$$
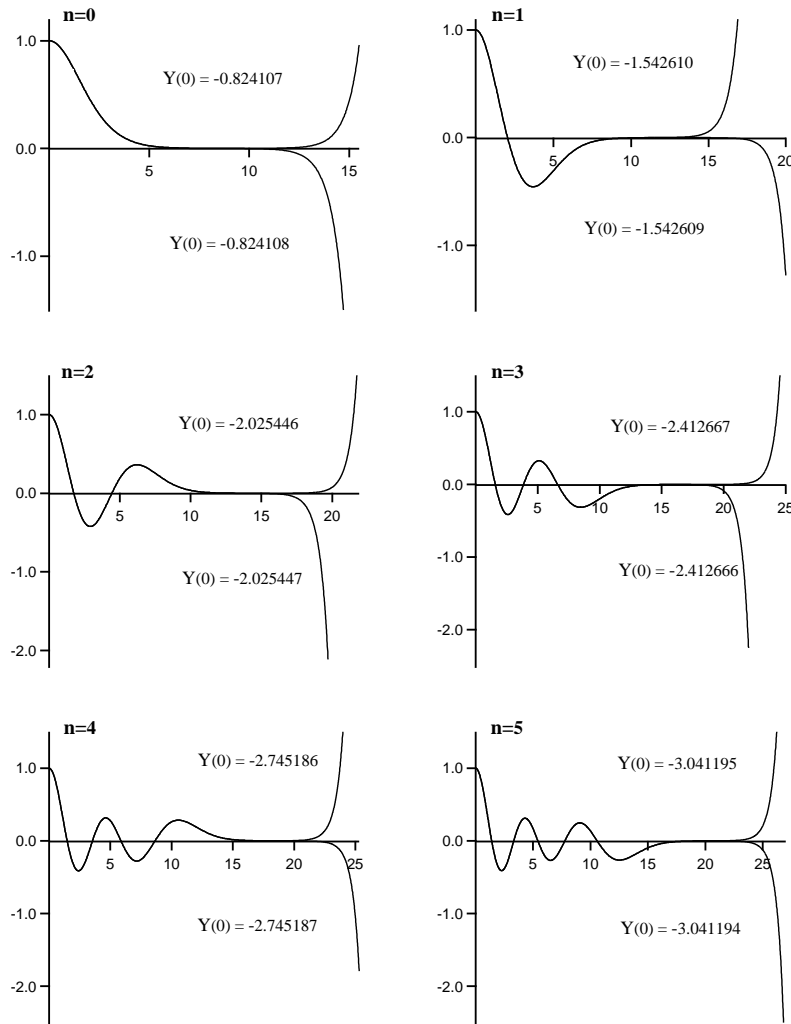
Figure 2.4: the solutions Ψ of Eqs. (2.2-2) and (2.3) with $\Psi(0) = 1$

From $Y(r) = \lambda^2 \widetilde{Y}(\lambda r)$, one has

$$Y(r) \to C \ln r + D \quad \text{as } r \to \infty, \tag{2.20}$$

where

$$C = \frac{\lambda^2}{2\pi}, \quad D = \lambda^2 \left(\frac{\ln \lambda}{2\pi} - \omega \right). \tag{2.21}$$

Since C and D can be obtained by fitting the values of the bound-state solutions Y at large r, one

Table 3: Values of $Y_n(0)$, C_n, and D_n for the 2-D case

n	$Y_n(0)$	C_n	D_n
0	-0.82411	1.35273	-1.14255
1	-1.54261	2.40683	-4.03590
2	-2.02545	3.13053	-6.45050
3	-2.41267	3.71589	-8.59419
4	-2.74519	4.22061	-10.5565
5	-3.04119	4.67094	-12.3853

Table 4: Values of λ_n, ω_n, $\widetilde{\Psi}_n(0)$, and $\widetilde{V}_n(0)$ for the 2-D case

n	$\lambda_n = (2\pi C_n)^{1/2}$	$\omega_n = (4\pi)^{-1}\ln(2\pi C_n)$ $-D_n(2\pi C_n)^{-1}$	$\widetilde{\Psi}_n(0) = (2\pi C_n)^{-1}$	$\widetilde{V}_n(0) = (4\pi)^{-1}\ln(2\pi C_n)$ $+[Y_n(0) - D_n](2\pi C_n)^{-1}$
0	2.9154	0.3047	0.1177	0.2078
1	3.8888	0.4830	0.0661	0.3810
2	4.4351	0.5650	0.0508	0.4620
3	4.8319	0.6188	0.0428	0.5155
4	5.1496	0.6589	0.0377	0.5554
5	5.4174	0.6909	0.0341	0.5873

obtains the scaling constant λ and the eigenvalue ω. The values C and D for the n-th bound-state solution, $n = 0, 1, 2, 3, 4, 5$, are reported in the 2nd and 3rd columns of Table 3.

From Eq. (2.21) and $\Psi(0) = 1$, one has

$$\lambda = (2\pi C)^{1/2}, \tag{2.22}$$

$$\omega = \frac{\ln\lambda}{2\pi} - \frac{D}{\lambda^2}$$
$$= (4\pi)^{-1}\ln(2\pi C) - D(2\pi C)^{-1} \tag{2.23}$$

$$\widetilde{\Psi}(0) = \frac{1}{\lambda^2}\Psi(0) = (2\pi C)^{-1}, \tag{2.24}$$

$$\widetilde{Y}(0) = \frac{1}{\lambda^2}Y(0) = Y(0)(2\pi C)^{-1}. \tag{2.25}$$

Moreover,

$$\widetilde{V}(0) = \widetilde{Y}(0) + \omega$$
$$= (4\pi)^{-1}\ln(2\pi C) + [Y(0) - D](2\pi C)^{-1}. \tag{2.26}$$

The values λ, ω, $\widetilde{\Psi}(0)$, $\widetilde{V}(0)$ for the n-th bound-state solution, $n = 0, 1, 2, 3, 4, 5$, are reported in Table 4.

As shown in Figs. 2.1 and 2.3, rapidly increasing precision is required for the shooting parameter $Y(0)$ to extend the range of r before Ψ eventually diverges. In other words, the solution at large r is extremely sensitive to $Y(0)$. This makes it difficult to verify the convergence of the solutions at large r. On the contrary, for the boundary-value method the boundary conditions are enforced by the algorithm. The solution is stable with respect to small variation in the initial guesses. To find a convergent solution that extends to large r, the initial guesses only need to be in an appropriate neighborhood of the real solutions. The solutions for small r obtained by the shooting method serve well for this purpose.

3   Solutions by the Boundary-Value Method

In this section, the ordinary differential equations in Eq. (1.8) with the boundary conditions in Eqs. (1.9) and (1.12) will be solved by the boundary-value method. In the boundary-value method, a piecewise cubic polynomial function $S(r)$ is used, which satisfies the boundary conditions and, for a selected mesh $r_0 < r_1 < \cdots < r_N$, it collocates at the two end points of each subinterval $[r_i, r_{i+1}]$ [19]. In [20, 21] it is shown that this collocation method is equivalent to the 3-stage Lobatto IIIa implicit Runge-Kutta formula. The adaption of the mesh will be determined by the residual of $S(r)$ [22]. Since the algorithm must adjust the mesh and find $S(r)$ that matches the boundary conditions and gives a minimal residual, it is equivalent to a minimum-finding problem. Its difficulty lies in the need of an initial guess of the eigenvalues and the solutions that are close enough to the real solutions. As mentioned in section 2, the solution V is increasing for all r. For the ground-state solution, Ψ has no zeros and is decreasing for all r. The initial guess should be made to bear these properties. Moreover, we use the values λ_n, ω_n, and $\widetilde{\Psi}_n(0)$, $\widetilde{V}_n(0)$ in tables 2 and 4 as a guidance to the initial guess of the solutions. Within a neighborhood of those values, solutions that can be extended to arbitrarily large r are found.

3.1   The 1-dimensional case

For the 1-D case, one can use the following functions as the initial guess.

$$\Psi \;=\; ae^{-(r/\lambda)^2}, \tag{3.1}$$

$$V \;=\; be^{-r/b} + r, \tag{3.2}$$

where λ is the scaling parameter and $a = \Psi(0)$, $b = V(0)$ are the heights. The reason for this choice is that $\Psi = ae^{-(r/\lambda)^2}$ is a decreasing function, $V = be^{-r/b} + r$ is an increasing function, and they satisfy the smoothness condition in Eq. (1.9) and the boundary condition in Eq. (1.12-1). It turns out that we do not need a precise initial guess. Even though the guess in Eq. (3.1) has no zeros, it works also for the excited-state solutions. Using Eqs. (3.1) and (3.2) as the initial guess
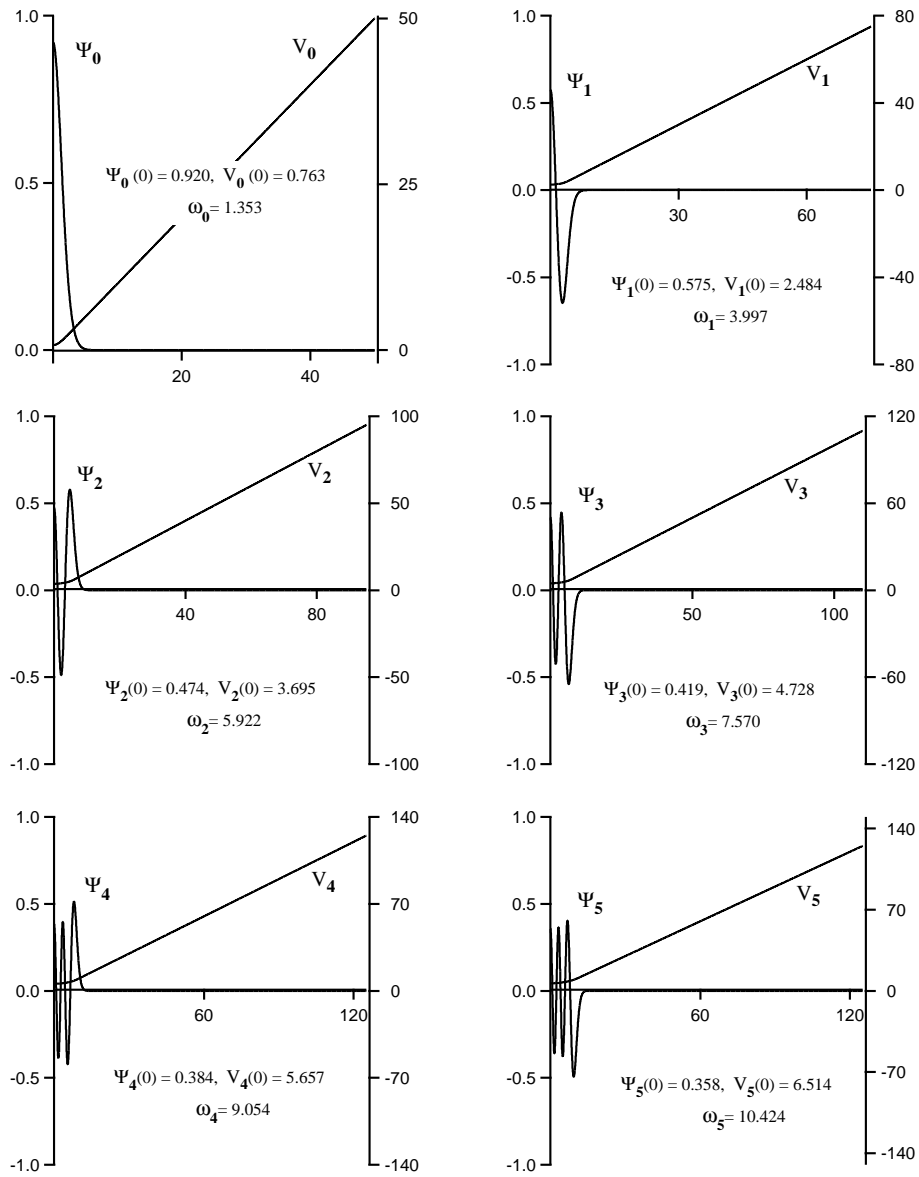
Figure 3.5: the solutions of the ground state and the first five excited states for the 1-D case

with λ, a, b, and the corresponding eigenvalue ω set to the values λ_n, $\widetilde{\Psi}_n(0)$, $\widetilde{V}_n(0)$, and ω_n in Table 2, we obtain the excited-state solutions as well as the ground-state solution. The solutions are shown in Fig. 3.5.

3.2 The 2-dimensional case

For the 2-D case, the following functions can be used as the initial guess for the ground state solution.

$$\Psi = ae^{-(r/\lambda)^2}, \tag{3.3}$$

$$V = \frac{1}{2\pi}\ln\left[r + e^{2\pi b}\exp\left(-\frac{r}{e^{2\pi b}}\right)\right], \tag{3.4}$$

where λ is the scaling parameter and $a = \Psi(0)$, $b = V(0)$. The reason for this choice is that $\Psi = ae^{-(r/\lambda)^2}$ is a decreasing function, $V = \frac{1}{2\pi}\ln\left[r + e^{2\pi b}\exp\left(-r/e^{2\pi b}\right)\right]$ is an increasing function, and they satisfy the smoothness condition in Eq. (1.9) and the boundary condition in Eq. (1.12-2). Different from the 1-D case, more elaborated functions are needed for the initial guess of excited-state solutions. The short-range solutions obtained by the shooting method can provide the guidance. The solutions obtained are shown in Fig. 3.6. Alternatively one can also use the inner-outer-iteration method which uses more iterations systematically to replace the requirement for more precise initial guesses. The method was developed to find 3-D stationary solutions with high efficiency [17].

4   Convergence at large distance

In both 1-D and 2-D cases, the solutions are computed in a finite interval $[0, r_{\max}]$ as shown in Figs. 3.5 and 3.6. Although in practice it is not possible to compute the solutions for $r_{\max} \to \infty$, it is essential to make sure that the integrated probability density beyond $r_{\max}$ is negligible and the variation of solutions as the result of choosing a larger $r_{\max}$ is also negligible. To facilitate the discussion, let us denote the nth solution on $[0, 2^k r_{\max}]$ as $\Psi_n^k(r)$. We study the convergence of the solutions for large r by computing $|\omega_n^{k+1} - \omega_n^k|$ and $\left(\Psi_n^{k+1} - \Psi_n^k\right)_{\mathrm{rms}}$ as $r_{\max}$ is doubled repeatedly, where for the 1-D case

$$\left(\Psi_n^{k+1} - \Psi_n^k\right)_{\mathrm{rms}} = \left[\frac{1}{2^k r_{\max}}\int_0^{2^k r_{\max}}\left|\Psi_n^{k+1}(r) - \Psi_n^k(r)\right|^2 dr\right]^{1/2} \tag{4.1-1}$$

and for the 2-D case

$$\left(\Psi_n^{k+1} - \Psi_n^k\right)_{\mathrm{rms}} = \left[\frac{1}{\pi(2^k r_{\max})^2}\int_0^{2^k r_{\max}}\left|\Psi_n^{k+1}(r) - \Psi_n^k(r)\right|^2 2\pi r dr\right]^{1/2}. \tag{4.1-2}$$

The results are that all the $|\omega_n^{k+1} - \omega_n^k|$ are below 10^{-16} and all the $\left(\Psi_n^{k+1} - \Psi_n^k\right)_{\mathrm{rms}}$ for the 1-D case are below the precision limit (10^{-12}) of the numerical integration in Eq. (4.1-1). For the 2-D case $\left(\Psi_n^{k+1} - \Psi_n^k\right)_{\mathrm{rms}}$ are shown in Table5. In all the cases as the range of integration is increased, $\left(\Psi_n^{k+1} - \Psi_n^k\right)_{\mathrm{rms}}$ does not increase. The results verify the convergence of the solutions for large r.
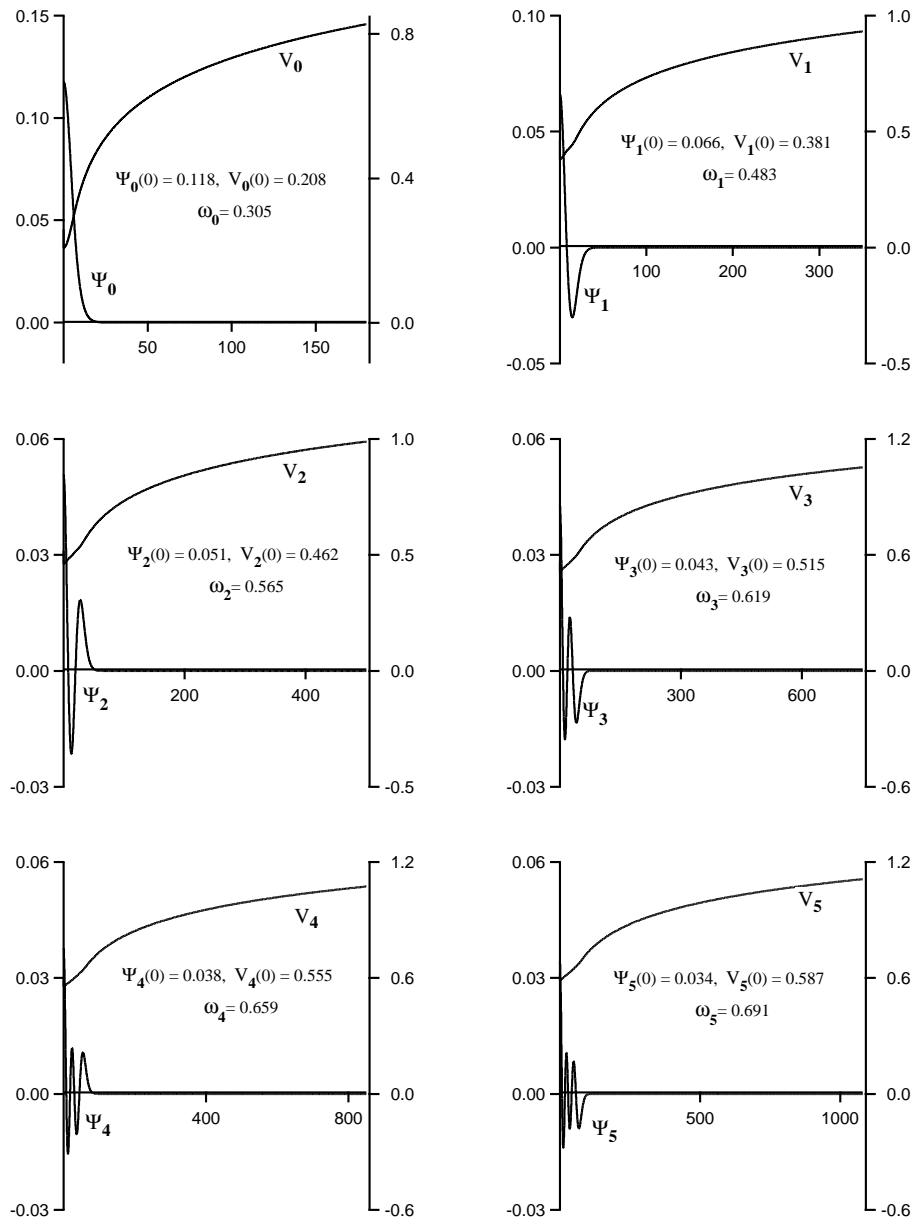
Figure 3.6: the solutions of the ground state and the first five excited states for the 2-D case

5 Summary

We have computed 1-D and 2-D solitary symmetric solutions of the attractive Schrödinger-Poisson equations using the shooting method and the boundary-value method. The solutions rep-

Table 5: the convergence of the 2-D solutions for large r

		$n = 0$ $r_{\max} = 175$	$n = 1$ $r_{\max} = 350$	$n = 2$ $r_{\max} = 500$	$n = 3$ $r_{\max} = 700$	$n = 4$ $r_{\max} = 800$	$n = 5$ $r_{\max} = 1000$
	$k = 0$	1.1×10^{-7}	6.9×10^{-8}	5.3×10^{-8}	3.8×10^{-8}	3.5×10^{-8}	2.8×10^{-8}
$\left(\Psi_n^{k+1} - \Psi_n^{k}\right)_{\mathrm{rms}},$	$k = 1$	3.9×10^{-8}	2.5×10^{-8}	1.7×10^{-8}	1.3×10^{-8}	1.2×10^{-8}	9.8×10^{-9}
	$k = 2$	1.4×10^{-8}	8.9×10^{-9}	6.6×10^{-9}	4.8×10^{-9}	4.4×10^{-9}	3.4×10^{-9}
	$k = 3$	5.1×10^{-9}	3.1×10^{-9}	2.4×10^{-9}	1.6×10^{-9}	1.5×10^{-9}	1.2×10^{-9}

resent the self-gravitating effect of massive sheets for the 1-D case and massive wires for the 2-D case. It is shown that the shooting method can be used to find the solutions in the short range efficiently, but not in the long range because of its inherent sensitivity to the initial conditions. Whereas the boundary-value method can be used to compute the solutions in the full range efficiently if the short range solutions provided by the shooting method is used as the initial guesses. In this way the two methods complement each other. Convergence analysis shows that the solutions fall off fast enough so that they represent truly localized solutions.

References

[1] D. J. Kaup (1968), *Klein-Gordon Geon,* Phys. Rev. **172**, 1331.

[2] R. Ruffini and S. Bonazzola (1969), "Systems of self-gravitating particles in general relativity and concept of an equation of state", *Phys. Rev.* **187**, 1767.

[3] R. Friedberg, T. D. Lee, and Y. Pang (1987), "Scalar soliton stars and black holes", *Phys. Rev. D* **35**, 3640.

[4] F. E. Schunck and E. W. Mielke (2003), "General relativistic boson stars", *Class. Quantum Grav.* **20** , R301.

[5] P. A. Markowich, C. Ringhofer, and C. Schmeiser (1990), "Semiconductor Equations", *Springer-Verlag*.

[6] F. Nier (1990), "A stationary Schrödinger-Poisson system arising from the modelling of electronic devices", *Forum Math* **2**, 489.

[7] F. Nier (1993), "A variational formulation of Schrödinger-Poisson systems in dimension D-less-than-or-equal-to-3", *Commun. Partial Differential Equations* **18**, 1125.

[8] F. Nier (1993), "Schrödinger-Poisson systems in dimension D-less-than-or-equal-to-3-the whole-space case", *Proceedings of the Royal Society of Edinburgh* **123A**, 1179.

[9] H. C. Kaiser and J. Rehberg (1997), "On stationary Schrödinger-Poisson equations modelling an electron gas with reduced dimension", *Math. Meth. Appl. Sci.* **20**, 1283.

[10] R. Illner, P. F. Zweifel, and H. Lange (1994), "Global existence, uniqueness and asymptotic-behavior of solutions of the Wigner-Poisson and Schrödinger-Poisson systems", *Math. Meth. Appl. Sci.* **17** , 349.

[11] Óscar Sánchez and J. Soler (2004), "Asymptotic decay estimates for the repulsive Schrödinger-Poisson system", *Math. Meth. Appl. Sci.* **27**, 371.

[12] R. T. Glassey (1977), "Asymptotic behavior of solutions to certain nonlinear Schrödinger-Hartree equations", *Commun. Math. Phys.* **53**, 9.

[13] E. R. Arriola and J. Soler (1999), "Asymptotic behavior for the 3-D Schrödinger-Poisson system in the attractive case with positive energy", *Appl. Math. Lett.* **12**, 1.

[14] E. R. Arriola and J. Soler (2001), "A variational approach to the Schrödinger-Poisson system: Asymptotic behavior, breathers, and stability", *J. Stat. Phys.* **103**, 1069.

[15] P. Tod and I. M. Moroz (1999), "An analytical approach to the Schrödinger-Newton equations", *Nonlinearity* **12**, 201.

[16] I. M. Moroz, R. Penrose, and P. Tod (1998), "Spherically-symmetric solutions of the Schrödinger-Newton equations", *Class. Quantum Grav.* **15**, 2733.

[17] D. H. Bernstein, E. Giladi, K. R. W. Jones (1998), "Eigenstates of the gravitational Schrödinger equation", *Mod. Phys. Lett. A* **13**, 2327.

[18] K. P. Tod (2001), "The ground state energy of the Schrödinger-Newton equation", *Physics Letters A* **280**, 173.

[19] E. Dickmanns and K. Well (1975), "Approximate solution of optimal control problems using third order Hermite polynomial functions", in Optimization Techniques, G. I. Marchuk, ed., vol. **27** of Lecture Notes in Computer Science, *Springer*, pp. 158-166.

[20] J. R. Cash (1988), "On the numerical integration of nonlinear two-point boundary value problems using iterated deferred corrections. part 2: the development and analysis of highly stable deferred correction formulae", *SIAM J. Numer. Anal.* **25**, 862.

[21] S. Gupta (1985), "An adaptive boundary value Runge   Kutta solver for first order boundary value problems", *SIAM J. Numer. Anal.* **22**, 114.

[22] W. H. Enright and P. H. Muir (1996), "Runge-Kutta software with defect control for boundary value ODEs", *SIAM J. Sci. Comput.* **17**, 479.

薛丁格─帕松方程式的一維和二維解

曹景懿[*]

摘　　要

　　薛丁格─帕松方程式是一組非線性微分方程式，很多重要的物理問題是以它為骨幹。其中一個令我們感興趣的問題是重力在量子力學中的效應。由波函數所描述的物質密度分佈透過帕松方程式來決定重力位能，而位能又反過來經由薛丁格方程式改變物體的波函數。這樣的反饋作用將非線性效應引進了量子力學中，這些非線性效應具有豐富的數學結構待探索。

　　最簡單例子是三度空間中 (1) 單一質點，系統的方程式是三維球對稱；(2) 在 z 方向的一條質量線，系統的方程式變成二維柱對稱；(3) 在 y-z 平面上的一個質量面，系統的方程式變成一維。我利用兩種數值方法來研究這些方程式的解，計算它的能譜和對應波函數的寬度及高度的尺度變化。第一種方法是根基於標準的四階 Runge-Kutta 演算法的 shooting approach，第二種方法是根基於三階段 Lobatto IIIa 隱性 Runge-Kutta 公式和適應性格點的 boundary-value-problem (BVP) approach。第一種方法 shooting approach 可將問題簡化成一維的搜尋，藉著調整位能的初始值來找尋符合邊界條件的解。但是因為解在邊界的行為會隨著初始值劇烈變化，所以此種方法只在短距離內有效。第二種方法 BVP approach 是將邊界條件直接內建於程式之中，它的困難在於需要一個相當接近真正解的初始猜測解，來保障一個收斂的過程，所以我用第一種方法找到的短距離解來輔助猜測，兩種方法相輔相成。

　　無論用 shooting approach 或 BVP approach，邊界都不可能真的設在無窮遠，因此找到解之後，我們會以幾何倍率擴大解的範圍，以確認它在遠處的收斂性。

關鍵詞：薛丁格方程式，帕松方程式。

[*] 東海大學數學系